Earth and Planetary Science Letters 460 (2017) 12–21

Contents lists available at ScienceDirect

Earth and Planetary Science Letters

www.elsevier.com/locate/epsl

Crustal mechanics control the geometry of mountain belts. Insights from numerical modelling

Katharina Vogt *, Liviu Matenco, Sierd Cloetingh

Department of Earth Sciences, Utrecht University, Budapestlaan 6, 3584 CD Utrecht, Netherlands

ARTICLE INFO

Article history:
Received 6 June 2016
Received in revised form 28 October 2016
Accepted 8 November 2016
Available online xxxx
Editor: A. Yin

Keywords:
collision
mountain belt
continental subduction
double vergent orogen
numerical modelling

ABSTRACT

Continental collision forms mountain ranges that have shaped much of Earth's topography. Yet, the process by which material is transported and redistributed in collision zones remains debatable. Here we present a series of two-dimensional thermo-mechanical experiments on continent–continent collision zones to investigate the role of crustal strength in terms of geometry, deformation and exhumation. Depending on the crustal rheology, rate of collision and initial temperature distribution, continental collision may form double vergent orogens or result in continental subduction. Double vergent orogens are characterized by subduction of the lithospheric mantle, diffuse fore- and highly localized retro-shears, elevated topographies, and exhumation of high grade metamorphic rocks. In contrast, continental subduction results in subduction of lower continental crust, the formation of a wedge shaped Moho, a foreland propagating deformation zone, "lower" topographic build-up and exhumation of low grade metamorphic rocks. It is the combination of strength variations and ambient conditions that determines the geometry of mountain belts. Strong rheological coupling of upper and lower crust forms double vergent orogens; low rheological coupling of upper and lower crust results in continental subduction.

1. Introduction

When continents collide mountain ranges with high topographies and complex (internal) geometries are formed. Tectonically induced stresses result in intense deformation with crustal thrusting being the primary response. Hence, crustal material is transported and redistributed within an orogen, destroying its original rock sequence. Constraints on the final crustal architecture come from surface geology, deep seismic reflection profiles and teleseismic tomography, but the mechanism that lead to its final structure remain debatable.

Early analytical (Davis et al., 1983), analogue (Malavieille, 1984) and numerical studies (Willett et al., 1993; Beaumont et al., 1996) of orogeny have focused solely on the frictional (plastic) behaviour of the continental crust, by applying a local velocity condition at its base. The resulting crustal structure is highly asymmetric with strain being more diffuse in the foreland and highly localized in the hinterland. Typical examples to which these models have successfully been applied include the Swiss Alps, the New Zealand Alps and the Pyrenees (e.g.: Beaumont et al., 1996; Jammes and Huismans, 2012; Erdős et al., 2014). The deformation pattern in such type of experiments is strongly conditioned by the velocity discontinuity at the base of the crust that excludes any involvement of mantle lithosphere. Several studies have subsequently explored the impact of thermally activated viscous creep and plastic yielding using a similar setup (Beaumont and Quinlan, 1994; Willett, 1999; Pfiffner et al., 2000; Ellis et al., 2001), but the geometry of the resulting orogen is comparable to previous models using similar boundary conditions.

More recent analogue modelling studies have challenged this idea by demonstrating that deformation might be restricted to the lower plate and lack any retro-wedge formation (Willingshofer et al., 2013). Similar results where obtained from numerical simulations performed on a lithospheric scale that have stressed the importance of rheological stratification on the relationship between subduction of continental lithosphere, strain distribution and the resulting geometry of the collisional orogen (Jammes and Huismans, 2012; Erdős et al., 2014). Common examples of orogens, where no significant upper plate deformation has been observed include the Carpathians (Matenco et al., 2010), the Apennines (Carminati and Doglioni, 2012), parts of the Greater Caucasus (Forte et al., 2014), and the South East Asia collisional zones (Morley, 2012).

* Corresponding author.
E-mail address: k.j.vogt@uu.nl (K. Vogt).

http://dx.doi.org/10.1016/j.epsl.2016.11.016
0012-821X/

Table 1
Material properties. ρ = initial density. Wet qtz = wet quarzite, plag = plagioclase (anorthite 75%), dry ol = dry olivine, wet ol = wet olivine after Ranalli (1995) and references therein. A_D is the pre-exponential factor, n, is the stress exponent, E_a is the activation energy, V_a is the activation volume, ϕ is the friction angle, and C is the cohesion. Strain weakening is applied within a strain interval of 0–1 at which the friction angle ($sin(\phi)$) and cohesion (C) are decreased. H_r = radioactive heat production, C_p = isobaric heat capacity, α = coefficient of thermal expansion, β = coefficient of thermal compressibility, k = thermal conductivity, $A = T[K] + 77$, $B = 0.00004 \times P$ [MPa].

Material properties:	Sediment	Upper crust decoupled	Upper crust coupled	Lower crust	Mantle	Weak shear zone
ρ [kg/m^3]	2600	2700	2700	2900	3300	3200
Flow law	wet qtz	wet qtz	plag	plag	dry ol	wet ol
$1/A_D$ [Pa^n s]	1.97×10^{17}	1.97×10^{17}	4.80×10^{22}	4.80×10^{22}	3.98×10^{16}	5.01×10^{20}
n	2.3	2.3	3.2	3.2	3.5	4.0
E_a [J]	154×10^3	154×10^3	238×10^3	238×10^3	532×10^3	470×10^3
V_a [J/bar]	0.8	0.8	0.8	0.8	0.8	0.8
$sin(\phi)$	0.20–0.10	0.30–0.15	0.30–0.15	0.30–0.15	0.60–0.30	0.10–0.05
c [Pa]	$1 \times 10^{7-6}$	$1 \times 10^{7-6}$	$1 \times 10^{7-6}$	$1 \times 10^{7-6}$	$1 \times 10^{7-6}$	$1 \times 10^{7-6}$
H_r [μW/m^3]	2.0	1.8	1.8	0.18	0.022	0.022
C_p [J/kg K]	1000	1000	1000	1000	1000	1000
α [1/K]	3×10^{-5}	3×10^{-5}	3×10^{-5}	3×10^{-5}	3×10^{-5}	3×10^{-5}
β [1/MPa]	1×10^{-5}	1×10^{-5}	1×10^{-5}	1×10^{-5}	1×10^{-5}	1×10^{-5}
k [W/m/K]	$[0.64 + 807/A]$ $\times \exp(B)$	$[0.64 + 807/A]$ $\times \exp(B)$	$[0.64 + 807/A]$ $\times \exp(B)$	$[1.18 + 474/A]$ $\times \exp(1 + B)$	$[0.73 + 1293/A]$ $\times \exp(1 + B)$	$[0.73 + 1293/A]$ $\times \exp(1 + B)$

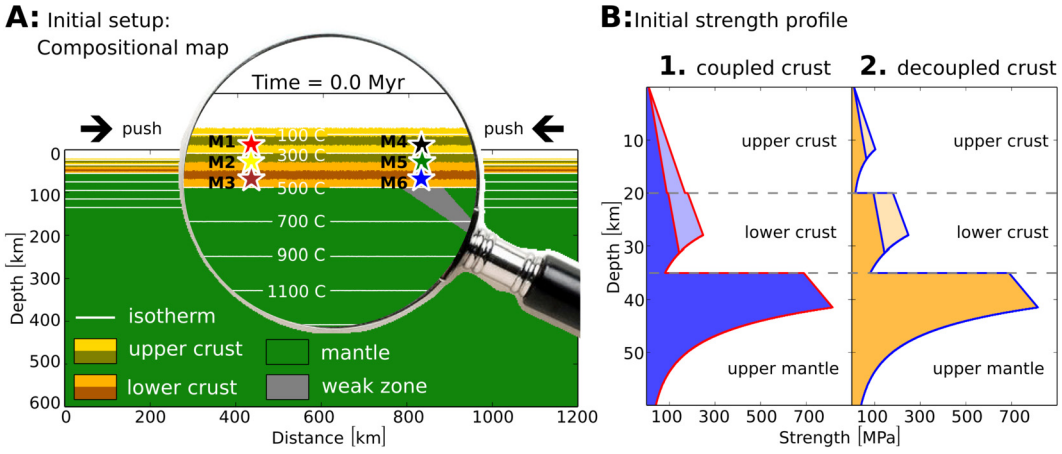

Fig. 1. A: Cross-section of the initial setup. M1–M6 (stars) denote markers (rocks) that have been traced through space and time to compute pressure–temperature paths. **B:** Initial strength profile of the continental lithosphere for a constant strain rate of $\dot{\varepsilon} = 10^{-14}$ s^{-1}. Two initial strength profiles are used: coupled and decoupled crust (left and right, respectively). Strain weakening is applied within a strain interval of 0–1, which results in lower plastic strength. The light blue and yellow colours mark the initial crustal strength of the model. The dark blue and yellow colour mark the crustal strength of the model after strain weakening. See Table 1 for all material properties. (For interpretation of the references to colour in this figure, the reader is referred to the web version of this article.)

In this study we use numerical high-resolution thermo-mechanical models to investigate the impact of crustal rheology upon continental collision. We show that the strength distribution within the continental crust imposes major implications on the mode of deformation, the final crustal architecture and the exhumation pattern.

2. Methods

All numerical experiments were performed with the I2VIS code (Gerya and Yuen, 2003). This code is based on conservative finite differences and a marker-in-cell technique. The momentum, continuity and energy equations are solved on an Eulerian frame. Physical properties are transported by Lagrangian markers that move according to the velocity field interpolated from the fix grid. The model uses non-Newtonian visco-plastic rheologies to simulate multiphase flow (Table 1) and is designed to study the dynamic processes during continental collision.

2.1. Model setup

The computational domain is two-dimensional and covers 1200 km × 600 km with a resolution of 1391 × 451 nodal points (Fig. 1). The spacing of the gridlines increases from 10 × 4 km to 0.5 × 0.5 km toward the centre of the domain, where highest deformation occurs, i.e. area of orogeny (500 km × 100 km) (Gerya, 2010b). The left, right and upper boundary of the model are free slip. The lower boundary is open and satisfies an external free slip boundary condition below the box at 996 km depth (Gerya, 2010b).

The continental crust is homogeneous and has a total thickness of 35 km. It is subdivided into 20 km of felsic and 15 km of mafic rocks. The underlying mantle is composed of dry olivine. An internally prescribed velocity field within the convergence condition region ensures horizontal compression between two continental blocks, representing collision. A weak zone with low plastic strength and wet olivine rheology at the bottom of the continental crust represents a suture zone, separating two continental domains after the closure of an ocean (Fig. 1). This suture zone provides efficient decoupling between the colliding plates and enables subduction of the incoming mantle lithosphere beneath the collisional orogen (Burg and Gerya, 2005; Willingshofer et al., 2013).

The thermal boundary conditions are 0 °C at the upper boundary and 0 heat flux across the vertical boundaries. A thermal gradient of 25 °C/km is used for the uppermost 10 km of the continental lithosphere, followed by a lower gradient of 10 °C/km until a temperature of 1330 °C at the lithosphere–asthenosphere boundary is reached. This initial gradient results in a Moho-